

COLOR IMAGE INDEXING USING MATHEMATICAL MORPHOLOGY

CONTENTS

1. Introduction	1
2. Preliminaries	1
2.1. Norms and distances	1
2.2. Color space representations	2
2.3. Color distances	3
3. Distances-based morphological color operators	3
3.1. Total orderings using distances completed with cascades	3
3.2. Morphological color operators	4
4. Experimental results for distances-based morphological color operators	4
5. Morphological image indexing based on edge extraction	5
References	7

COLOR IMAGE INDEXING USING MATHEMATICAL MORPHOLOGY - PRELIMINARY STUDY -

Eugen ZAHARESCU
MFP - Bilkent University of Ankara
ezaharescu@ee.bilkent.edu.tr

1. Introduction

The extension of mathematical morphology operators to multi-valued functions, and in particular to color images, is neither direct nor general. In this paper I proposed a generalization of distance-based and lexicographical-based approaches, allowing the extension of morphological operators to color images for any color representation (e.g. *RGB*, *LSH* and *L*a*b**) and for any metric distance to a reference color. The performance of these morphological color operators will be illustrated by means of two applications: color image segmentation and indexing.

Mathematical morphology is the application of lattice theory to spatial structures [12], in practice, the definition of morphological operators needs a totally ordered complete lattice structure, i.e., the possibility of defining an ordering relationship between the points to be processed. Therefore, the application of mathematical morphology to color images is difficult due to the vectorial nature of the color data. Fundamental references to works which have formalized the vector morphology theory are [14] [4] [17]. In the literature, many techniques have been proposed on the extension of mathematical morphology to color images according to different orderings. The **marginal ordering** or **M-ordering** is an ordering based on the usual point wise ordering (i.e., component by component independently). An other more interesting one is called **conditional ordering** or **C-ordering**, where the vectors are ordered by means of some marginal components selected sequentially according to different conditions (i.e. **lexicographic ordering**). The **reduced ordering** or **R-ordering** performs the ordering of vectors according to some scalars, computed from the components of each vector with respect to different measure criteria, typically distances or projections. Using an **M-ordering**, we can introduce color vector values in the transformed image that are not present in the input image ("false colors") [14]. The application of **C-ordering** or **R-ordering** preserves the input color vectors and therefore is preferable for filtering applications. The **C-ordering** has been widely studied in the framework of color morphology, especially in a luminance/saturation/hue representation [9] [17] [5] [2]. The **R-ordering** has been used to define morphological operators by means of distances in [4]. In [11] was proposed a combination of an **R-ordering** and a **C-ordering**, in fact my approach can be considered as a generalization of this interesting study.

The aim of the first part of the paper is just to generalize the distance-based approaches and the lexicographical approaches in order to propose a general framework allowing the extension of morphological operators to color images for any color representation and for any metric distance. In fact, we introduce a generalization of mathematical morphology to multivariate functions according to a distance-to-origin-based interpretation of the notion of total ordering between the points of a complete lattice. In the second part of this study is considered the application of morphological color operators to color image segmentation and indexing.

2. Preliminaries

2.1. Norms and distances

Given an n -dimensional vector $x=(x_1, x_2, \dots, x_n)$, $x \in \mathbb{X}^n$ or $x \in \mathbb{P}^n$, a vector norm $\|x\|$ defined for x is a non-negative number (i.e., a function $\mathbb{P}^n \rightarrow \mathbb{P}_+$) satisfying the following three axioms: **1)** $\|x\| > 0$ when $x \neq 0$ and $\|x\| = 0$ iff $x = 0$; **2)** $\|kx\| = |k| \cdot \|x\|$ for any scalar k ; **3)** $\|x + y\| \leq \|x\| + \|y\|$. The most common norm is the L_2 norm or Euclidean norm, defined by $\|x\|_2 = \sqrt{\sum_{k=1}^n |x_k|^2}$, where $|x_k|$ denotes the complex modulus or the absolute value. The L_1 norm of a complex vector x is given by $\|x\|_1 = \sum_{k=1}^n |x_k|$. The third classical norm to be consider here is the L_∞ which is defined by $\|x\|_\infty = \max_{k, 1 \leq k \leq n} |x_k|$. Given two real vectors x and y , the distance metric between the two points, denoted by $d(x, y)$, is the mapping $d : \mathbb{P}^n \times \mathbb{P}^n \rightarrow \mathbb{P}_+$ which satisfies the following properties: **1) non-negativity** ($d(x, y) \geq 0$), and identity $d(x, y) \geq 0 \Leftrightarrow x = y$, **2) commutability** ($d(x, y) = d(y, x)$) and **3) triangular inequality** ($d(x, z) \leq d(x, y) + d(y, z)$). In fact, a metric distance can be defined based on each vector norm proposed, hence the distance between two vectors is the norm of the difference, i.e. $d(x, y) = \|x - y\|$. The L_2 norm distance is the **Euclidean distance**. The L_1 and L_∞ norm distances are also called the **Manhattan distance** and the **maximum distance**, respectively. The **Mahalanobis distance** is a special case of the quadratic-form generalized distance metric in which the transform matrix is given by the

covariance matrix Γ obtained from a training set of data that represents the reliability or scale of the measurement in each direction. The *Mahalanobis distance* between two vectors is given by $\|\mathbf{x} - \mathbf{y}\|_M = (\mathbf{x} - \mathbf{y})^T \Gamma^{-1} (\mathbf{x} - \mathbf{y})$. It must be reminded that if \mathbf{x} and \mathbf{y} are n -dimensional vectors then the covariance matrix Γ is an $n \times n$ matrix. In the special case when all the vector components are statistically independent, but have unequal variances σ_k^2 , Γ is a diagonal matrix. In

this case, the Mahalanobis distance reduces to $\|\mathbf{x} - \mathbf{y}\|_M = \sum_{k=1}^n \frac{(x_k - y_k)^2}{\sigma_k^2}$

2.2. Color space representations

The first issue to be addressed in order to apply mathematical morphology to color images is the color space representation. The most direct way to manipulate digital color images is to work on the **RGB** color space (the usual sensors in digital cameras are **RGB** CCD's). A color image \mathbf{f} is a vector function $\mathbf{f}(\mathbf{x}) = (f_R(\mathbf{x}), f_G(\mathbf{x}), f_B(\mathbf{x})) \in \mathbf{Z}^3$, $\mathbf{x} \in \mathbf{Z}^2$, where $f_R(\mathbf{x})$, $f_G(\mathbf{x})$, $f_B(\mathbf{x})$ are, respectively, the red, green, and blue channels at point \mathbf{x} .

However, the **RGB** color representation has some drawbacks: components are strongly correlated, lack of human interpretation, non uniformity, etc. A polar representation with the variables luminance, saturation et hue (lum/sat/hue) allows us to solve these problems. The **HLS** system is the most popular lum/sat/hue triplet. In spite of its popularity, the **HLS** representation (and other classical ones like **HSV**) often yields unsatisfactory results, for quantitative processing at least, because its luminance and saturation expressions are not norms, so average values, or distances, are falsified. In addition, these two components are not independent, which is a drawback for vector decomposition. The comprehensive analysis of this question was done by *Serra* [16]. The drawbacks of the **HLS** system can be overcome by various alternative representations, according to different norms used to define the luminance and the saturation. The L_I norm system has already been introduced in [15, 1] as follows:

$$\begin{cases} l = \frac{1}{3}(max + med + min) \\ s = \begin{cases} \frac{3}{2}(max - l) & \text{if } l \geq med \\ \frac{3}{2}(l - max) & \text{if } l \leq med \end{cases} \\ h = k \left[\lambda + \frac{1}{2} - \frac{(-1)^l}{2s}(max + min - 2med) \right] \end{cases}$$

where max , med and min refer the maximum, the median and the minimum of the **RGB** color of the current point (r, g, b) , k is the angle unit ($\pi/3$ for radians and 42 to work on 256 grey levels) and $\lambda=0$, if $r > g \geq b$; 1 , if $g \geq r > b$; 2 , if $g > b \geq r$; 3 , if $b \geq g > r$; 4 , if $b > r \geq g$; 5 , if $r \geq b > g$ allows to change to the color sector. For each pixel, the luminance (or brightness) represents the total quantity of the intensity of light, the saturation represents a measurement of purity of the color, and the hue is an index representing the dominant wavelength (perceived color) of the light.

We can also compare it with the $L^*a^*b^*$ color space, the classical representation in colorimetry. The principal advantage of the $L^*a^*b^*$ space is its perceptual uniformity. However, the transformation from **RGB** to $L^*a^*b^*$ space is done by first transforming to the **XYZ** space, and then to the $L^*a^*b^*$ space [19]. The **XYZ** coordinates are depending on the device-specific **RGB** primaries and on the white point of illuminant. In most of situations, the illumination conditions are unknown and therefore a hypothesis must be made.

If the most common option, the **CIE D₆₅** daylight illuminant, is chosen then the exact calculations are:

$$\begin{cases} L^* = \begin{cases} 116 \left(\frac{Y}{Y_n} \right)^{\frac{1}{3}} - 16 & \text{if } \frac{Y}{Y_n} > 0.008856 \\ 903.3 \left(\frac{Y}{Y_n} \right) & \text{if } \frac{Y}{Y_n} \leq 0.008856 \end{cases} \\ a^* = 500 \left[f \left(\frac{X}{X_n} \right) - f \left(\frac{Y}{Y_n} \right) \right] \\ b^* = 200 \left[f \left(\frac{Y}{Y_n} \right) - f \left(\frac{Z}{Z_n} \right) \right] \end{cases}$$

where $f \left(\frac{\lambda}{\lambda_n} \right) = \left(\frac{\lambda}{\lambda_n} \right)^{\frac{1}{3}}$, if $\frac{\lambda}{\lambda_n} > 0.008856$ or $f \left(\frac{\lambda}{\lambda_n} \right) = 7.787 \left(\frac{\lambda}{\lambda_n} \right) + \frac{16}{116}$, if $\frac{\lambda}{\lambda_n} \leq 0.008856$. The symbol λ

represents X , Y or Z (the tristimulus values of the sample) and X_n , Y_n or Z_n are the tristimulus values of the adapting reference white point, i.e., for CIE D_{65} daylight illuminant are $X_n = 0.950$; $Y_n = 1.000$; $Z_n = 1.089$. The L^* coordinate provides a correlate to perceived lightness. The a^* and b^* coordinates approximate respectively the red-green and yellow-blue of an opponent color space. Achromatic stimuli, such as *whites*, *grays* and *blacks* have values of 0 for both a^* and b^* .

Let $f = (f_R, f_G, f_B)$ be a color image. Then its grey-level components in the improved LSH color space are (f_L, f_S, f_H) and in the $L^*a^*b^*$ color space are $(f_{L^*}, f_{a^*}, f_{b^*})$.

2.3. Color distances

Let $c_k = (c_k^U, c_k^V, c_k^W)$ be the color point k in any generic color space UVW (e.g. in LSH $c_k = (c_k^L, c_k^S, c_k^H)$). We can now define the color distance between two color vectors i and j as $\|c_i - c_j\|_{\Delta}^{UVW}$ where Δ is a particular metric. The four metric distances above recalled can be applied to color vectors according to the different color space representations, e.g. in RGB using L_2 we have $\|c_i - c_j\|_2^{RGB} = \sqrt{(c_i^R - c_j^R)^2 + (c_i^G - c_j^G)^2 + (c_i^B - c_j^B)^2}$. From the point of view of mathematical morphology, some issues must be taken into account. The value sets of functions associated to the RGB components, to the $L^*a^*b^*$ components and to the luminance and saturation components of the LSH representation are complete totally ordered lattices. The hue should be considered as a special case. The hue component is an angular function defined on the unit circle C , which has no partial ordering. For the hue, the angular difference [9, 6] is defined by $h_i \div h_j = |h_i - h_j|$, if $|h_i - h_j| \leq 180^\circ$ or $h_i \div h_j = 360^\circ - |h_i - h_j|$, if $|h_i - h_j| > 180^\circ$.

Therefore, for all the color metric distances in LSH , the term associated to the hue must use the angular difference, e.g. $\|c_i - c_j\|^{LSH} = |c_i^L - c_j^L| + |c_i^S - c_j^S| + |c_i^H \div c_j^H|$. On the other hand, it is well known the instability of the hue component for the low saturation points (this is an important issue to build hue-based distances, gradients, ordering, etc.). In order to cope with this drawback, the different solutions are generally based on a weighting of the hue by the saturation [3, 5, 2]. The simplest technique is to multiply the angular difference by the average saturation, i.e.

$$(1/2)(c_i^S - c_j^S) |c_i^H \div c_j^H|$$

As suggested in [3], other more sophisticated saturation-based weighing functions can be applied (e.g. sigmoid). Moreover, concerning the hue component manipulation, it is possible to fix an origin on the unit circle, denoted by h_0 . We can define now a h_0 -centered hue function by computing for each point i the value $(h_i \div h_0)(x) = h_i(x) \div h_0$. The co-domain set of this function $(h_i \div h_0)(x)$ is an ordered set and therefore leads to a complete totally ordered lattice.

Before applying these color distances to define morphological operators, a relevance analysis of the alternative distances shall be made. Firstly, the L_∞ norm distances could cause serious artifacts in the filtered color images because color vectors will be ordered according to only one of the components which can change for a set of points. It can be supposed that the results according to L_1 or L_2 will be relatively similar. In fact, the Mahalanobis distance can be interpreted as a generalization of them with the advantage of setting different weights for the components. Moreover it can be considered that, in the three color representations, the components are statistically independent and the Mahalanobis distance can be rewritten as a weighting distance, i.e.

$$\|c_i - c_j\|_{M(\omega_1, \omega_2, \omega_3)}^{UVW} = \omega_1 (c_i^U - c_j^U)^2 + \omega_2 (c_i^V - c_j^V)^2 + \omega_3 (c_i^W - c_j^W)^2.$$

3. Distances-based morphological color operators

The extension of morphological operators to color images based on lexicographical cascades from a LSH representation in norm L_1 is presented in references [1,2]. This approach is going further and is proposing a generic framework valid for any color representation and is adding the flexibility of a "reference color"-based morphology. In fact, after defining as reference the maximum gray value, the grayscale morphology can be interpreted in terms of distances to this reference: the *dilatation* δ tends to move toward this reference (i.e. δ is the value which have minimal distance to the reference within the structuring element) and the *erosion* ε away from it (i.e. ε is the value with maximal distance). This paradigm is directly applicable to color images (after fixing the color representation, the reference color c_0 and the color distance $\|\cdot\|$) by defining the following ordering for two color points: $c_i < c_j \Leftrightarrow \|c_i - c_0\| > \|c_j - c_0\|$. But this is only a partial ordering, i.e., two or more distinct color vectors within the structuring element can be equidistant from the reference. In order to have a total ordering, this primary reduced ordering must be completed with a lexicographical cascade.

3.1. Total orderings using distances completed with lexicographical cascades

The Ω -ordering or $<_\Omega$ is defined as: $c_i <_\Omega c_j$ iff:

$$\left\{ \begin{array}{l} \|c_i - c_0\|_{\Delta}^{UVW} > \|c_j - c_0\|_{\Delta}^{UVW} \text{ or} \\ \|c_i - c_0\|_{\Delta}^{UVW} = \|c_j - c_0\|_{\Delta}^{UVW} \text{ and} \\ \left\{ \begin{array}{l} c_i^V < c_j^V \text{ or} \\ c_i^V = c_j^V \text{ and } c_i^U < c_j^U \\ c_i^V = c_j^V \text{ and } c_i^U = c_j^U \text{ and } c_i^W < c_j^W \end{array} \right. \end{array} \right.$$

This lexicographical cascade is denoted compactly by $\Omega_{\Delta, c_0}^{UVW} \triangleright (V \rightarrow U \rightarrow W)$. In this case, the priority is given to the component V , then to U and finally to W . Obviously, it is possible to define other orders for imposing a dominant role to any other of the vector components. To simplify the number of alternatives, and based on the best results obtained from our previous works on lexicographical cascades, it is better to fix the ordering of the components for the three color spaces representations as follows: 1) $\triangleright (G \rightarrow R \rightarrow B)$, 2) $\triangleright (L \rightarrow S \rightarrow - (H \div h_0))$ (the origin of the hues correspond or is the same as for c_0) and 3) $\triangleright (L^* \rightarrow a^* \rightarrow b^*)$

3.2. Morphological color operators

Once these orderings have been established, the entire pyramid of the morphological color operators is defined in the standard way. The **color erosion** of an image f at pixel x by the structuring element B of size n is $\varepsilon_{\Omega, nB}(f)(x) = \{f(y) \mid f(y) = \inf_{\Omega}[f(z)], z \in n(B_x)\}$, where \inf_{Ω} is the infimum according to the total ordering Ω . The corresponding **color dilation** $\delta_{\Omega, nB}$ is obtained by replacing the \inf_{Ω} by the \sup_{Ω} , i.e., $\delta_{\Omega, nB}(f)(x) = \{f(y) \mid f(y) = \sup_{\Omega}[f(z)], z \in n(B_x)\}$. A **color opening** is an erosion followed by a dilation, i.e., $\gamma_{\Omega, nB}(f) = \delta_{\Omega, nB}(\varepsilon_{\Omega, nB}(f))$, and a **color closing** is a dilation followed by an erosion, i.e. $\varphi_{\Omega, nB}(f) = \varepsilon_{\Omega, nB}(\delta_{\Omega, nB}(f))$. Once the color opening and closing are defined it is obvious how to extend other classical operators like the alternate sequential filters, i.e. $ASF(f)_{\Omega, nB} = \varphi_{\Omega, nB} \gamma_{\Omega, nB} \cdot \cdot \cdot \varphi_{\Omega, 2B} \gamma_{\Omega, 2B} \varphi_{\Omega, B} \gamma_{\Omega, B}(f)$. Moreover, using a color distance (which can be different of the distance associated to the ordering Ω) to calculate the image distance d , given by difference point-by-point of two color images $d(x) = \|f(x), g(x)\|$, it is easy to define the **morphological gradient**, i.e., $\zeta_n(f) = \|\delta_{\Omega, nB}(f), \varepsilon_{\Omega, nB}(f)\|$, and the **top-hat transformation**, i.e., $\rho_{\Omega, nB}^+(f) = \|f, \gamma_{\Omega, nB}(f)\|$. In addition, the extension of the operators "by reconstruction" can be implemented using the **color geodesic dilation** which is based on restricting the iterative dilation of a **function marker** m by B to a function reference f [18], i.e., $\delta_{\Omega}^n(m, f) = \delta_{\Omega}^1 \delta_{\Omega}^{n-1}(m, f)$, where $\delta_{\Omega}^1(m, f) = \delta_{\Omega, B}(m) \wedge_{\Omega} f$. The **color reconstruction by dilation** is defined by $\gamma_{\Omega}^{\text{rec}}(m, f) = \delta_{\Omega}^i(m, f)$, such that $\delta_{\Omega}^i(m, f) = \delta_{\Omega}^{i+1}(m, f)$ (idempotence).

4. Experimental results for distances-based morphological color operators

In **figure 1** is given a comparison of the results obtained for a color opening by reconstruction $\gamma_{\Omega}(f)$ of the image "ChristmasTree". As we can observe, the results are absolutely different according to the distance-based total ordering chosen. Only examples for the L_2 and the **Mahalanobis** distance are shown. The orderings based on L_{∞} yield to very unsatisfactory visual results and the results for L_1 norm distances are almost equal to those for L_2 . Note also the flexibility of the approach, for instance, in **RGB** the result of the opening for L_2 distance to the origin (255,0,0) (pure red), which suppresses all the small red objects, is very different of the **Mahalanobis** distance with weights (1,0,0) (the R component is exclusively considered) to the same origin. On the other hand, we can observe that the orderings with distances including chromatic components (i.e. h, a^* and b^*) produce poor results. Moreover the choice of the origin is not easily understandable for the a^* and b^* components. Even if the Euclidean distance in the $L^*a^*b^*$ color space has interesting perceptual properties, we can remark that for the implementation of morphological operators the most important issue is in fact the choice of the origin. Hence, the use of the L_2 distance in **LSH** or $L^*a^*b^*$ should be considered for feature extraction operators according to a specific reference color. We can remark also that, in order to filter in a general way the structures of a natural color image, the opening to remove all the bright objects is visually better for $\|\bullet\|_2^{\text{RGB}}, c_0=(255,255,255)$ than for $\|\bullet\|_{M(I, I, \theta)}^{\text{LSH}}, c_0(255,255,-)$. The luminance and saturation components allow us therefore a better control of the significant components than the **RGB** components.



Figure 1.

Comparison of color opening by reconstruction $\gamma_{\Omega}(f)$ for the original image f "ChristmasTree" (the marker is an erosion $\epsilon_{\Omega,nB}(f)$ where the structuring element B is a square of size $n=20$) according to different distance-based total orderings.

5. Morphological image indexing based on edge extraction

One of the simplest morphological contour extraction methods is the morphological gradient: basically it consists of constructing an edge intensity map of the image as the difference between the local dilation and the local erosion at each image pixel (the word "local" being induced by the use of a structuring element with finite spatial support).

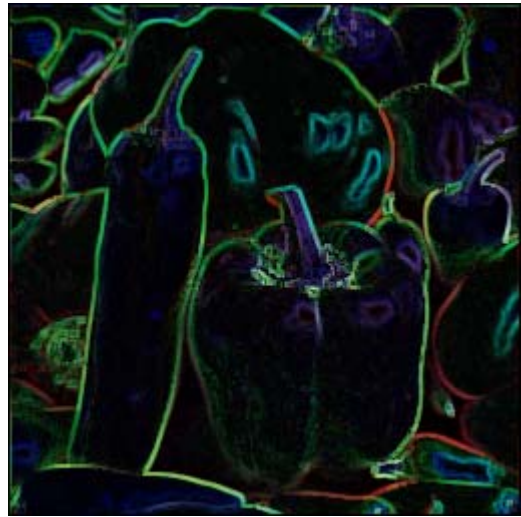
The edge intensity map consists of values proportional to the local variation within each pixel neighborhood, as defined by the support of the structuring element. The binary edge map is obtained by thresholding the edge intensity map and selecting the pixels with exhibit a strong color (value) variations, measured by important values of the morphological gradient.

A typical edge extraction result by the described method is presented in *figure 2*.



A

Original image
("peppers", 256 x 256 pixels)



B

Morphological gradient



C

Edge-intensity map extracted by the morphological gradient from the original image.



D

Binary contour map obtained by thresholding the edge-intensity map from figure 6. One can notice the good extraction of visual significant contours between different-colored components from the original "peppers" image.

Figure 2.

Morphological edge extraction for "peppers" image

In the end we can calculate a first geometric shape descriptor named *isoperimetric shape ratio*. This function is independent with respect to the scaling operations and is defined as the ratio between the surface and its squared perimeter of the objects in the binary contour map:

$$k = \frac{S}{P^2}$$

The *k*-ratio increases as the shape of the objects becomes more regular. *k* is maximum for a circular objects and decreases as the shape of the objects becomes linear. Although the *k*-ratio is not a bijective function this choice proved to be correct for reduced color ordering as it is dependent to the color hue and also luminance invariant by definition. The *isoperimetric shape ratio* can be calculated as a 3-component vector for corresponding to the 3 components of color space:

$$k = (k_l, k_s, k_h) = \left(\frac{S_l}{P_l^2}, \frac{S_s}{P_s^2}, \frac{S_h}{P_h^2} \right)$$

References:

- [1] J. Angulo, *Morphologie mathématique et indexation d'images couleur. Application a la microscopie en biomedecine*. Ph.D. Thesis, Ecole des Mines, Paris, December 2003.
- [2] J. Angulo, *Unified morphological color processing framework in a lum/sat/hue representation*, in Proc. of International Symposium on Mathematical Morphology (ISMM '05), Kluwer, 2005, 387-396.
- [3] T. Carron and P. Lambert, *Color edge detector using jointly Hue, Saturation and Intensity*, in Proc. of IEEE International Conference on Image Processing (ICIP'94), 1994, pp. 977-981.
- [4] J. Goutsias, H.J.A.M. Heijmans and K. Sivakumar, *Morphological Operators for Image Sequences*, Computer Vision and Image Understanding, 62(3) (1995) 326-346.
- [5] A. Hanbury and J. Serra, *Mathematical morphology in the HLS colour space*, in Proc. 12th British Machine Vision Conference (BMV'01), Manchester, 2001, pp. II-451-460.
- [6] A. Hanbury and J. Serra, *Morphological Operators on the Unit Circle*, IEEE Transactions on Image Processing, 10(12) (2001) 1842-1850.
- [7] H. Kramer and J. Bruckner, *Iterations of non-linear transformations for enhancement on digital images*, Pattern Recognition, 7, 1975, 53-58.
- [8] F. Meyer and J. Serra, *Contrasts and activity lattice*, Signal Processing, 16, 1989, 303-317.
- [9] R.A. Petters II, *Mathematical morphology for angle-valued images*, in Proc. of Non-Linear Image Processing VIII, 1997, Vol. SPIE 3026, 84-94.
- [10] S. Osher, L.I. Rudin, *Feature-oriented image enhancement using shock filters*, SIAM Journal of Numerical Analysis, 27, 1990, 919-940.
- [11] L.J. Sartor and A.R. Weeks, *Morphological operations on color images*, Electronic imaging, 2001, Vol. 10(2), 548-559.
- [12] J. Serra, *Image Analysis and Mathematical Morphology*. Vol I, and *Image Analysis and Mathematical Morphology*. Vol II: Theoretical Advances, London: Academic Press, 1982,1988.
- [13] J. Serra, *Toggle mappings*, in (Simon, Ed.) From Pixels to Features, 1989, North Holland, Amsterdam, 61-72.
- [14] J. Serra, *Anamorphoses and Function Lattices (Multivalued Morphology)*, in (Dougherty, Ed.) Mathematical Morphology in Image Processing, 1992, Marcel-Dekker, 483-523.
- [15] J. Serra, *Espaces couleur et traitement d'images*, CMM-Ecole des Mines de Paris, Internal Note N-34/02/MM, October 2002, 13 p.
- [16] J. Serra, *Morphological Segmentation of Colour Images by Merging of Partitions*, in Proc. of International Symposium on Mathematical Morphology (ISMM '05), Kluwer, 2005,151-176.
- [17] H. Talbot, C. Evans and R. Jones, *Complete ordering and multivariate mathematical morphology: Algorithms and applications*, in Proc. of the International Symposium on Mathematical Morphology (ISMM'98), Kluwer, 1998, 27-34.
- [18] L. Vincent, *Morphological Grayscale Reconstruction in Image Analysis: Applications and Efficient Algorithms*, IEEE Transactions on Image Processing, Vol. 2(2), 1993,176-201.
- [19] G. Wysecki and W.S. Stiles, *Color Science: Concepts and Methods, Quantitative Data and Formulae*, 2nd edition. John Wiley & Sons, New-York, 1982.